

# OXYGEN PLASMA MODIFICATION OF POSS-COATED KAPTON<sup>®</sup> HN FILMS

C. J. Wohl<sup>1,\*</sup>, M. A. Belcher<sup>2</sup>, S. Ghose<sup>2</sup>, J. W. Connell<sup>3</sup>

<sup>1</sup>NASA Postdoctoral Fellow at NASA Langley Research Center

<sup>2</sup>National Institute of Aerospace, Hampton, VA 23666-6147

<sup>3</sup>NASA Langley Research Center, Hampton, VA 23681-2199

## ABSTRACT

The surface energy of a material depends on both surface composition and topographic features. In an effort to modify the surface topography of Kapton<sup>®</sup> HN film, organic solutions of a polyhedral oligomeric silsesquioxane, octakis(dimethylsilyloxy)silsesquioxane (POSS), were spray-coated onto the Kapton<sup>®</sup> HN surface. Prior to POSS application, the Kapton<sup>®</sup> HN film was activated by exposure to radio frequency (RF)-generated oxygen plasma. After POSS deposition and solvent evaporation, the films were exposed to various durations of RF-generated oxygen plasma to create a topographically rich surface. The modified films were characterized using optical microscopy, attenuated total reflection infrared (ATR-IR) spectroscopy, and high-resolution scanning electron microscopy (HRSEM). The physical properties of the modified films will be presented.

This paper is work of the U.S. Government and is not subject to copyright protection in the U.S.

\* To whom correspondence should be addressed: [christopher.j.wohl@nasa.gov](mailto:christopher.j.wohl@nasa.gov), (757) 864-8074

KEY WORDS: Polyhedral Oligomeric Silsesquioxane, Lunar Dust, Surface Chemistry Modification

## 1. INTRODUCTION

NASA's existing Vision for Space Exploration (VSE) involves returning to the Moon with manned missions in 2020 [1]. Currently, there are several materials requirements for extended lunar missions that are of concern. Protection of astronauts and equipment from exposure to space-based radiation, efficient and cost-effective transport of materials to and from the Moon, and *in-situ* resource utilization (ISRU) to enable prolonged self-sustenance of lunar outposts are active areas of research. While lunar soil (regolith) covers the entire surface of the Moon and is being pursued as a resource (i.e., ISRU), it also presents a potential hazard to astronauts and equipment [2].

Regolith consists of a broad array of different sized particles with the micrometer sized portion (lunar dust) comprising a significant fraction that is potentially the most troublesome [3]. Lunar dust is produced from space weathering (meteorite impacts, radiation and thermal cycling) and, to a lesser degree, abrasion mechanisms due to the lunar surface dynamics of dust particles [4]. These processes also result in the formation of nano-scaled Fe<sup>0</sup> domains [5]. Although the Fe<sup>0</sup> oxidation state is not stable on Earth, the lack of atmosphere on the Moon enables these small magnetic domains to persist in lunar regolith. Exposure of lunar dust to solar radiation

causes ejection of electrons. The insulating nature of the dust particles results in generation of a positive surface potential which has been suggested to result in dust particle levitation and motion. The most significant movements are believed to occur at the terminator; the line separating the lunar day from lunar night [6]. Astronauts from the Apollo missions observed streaks in the sky near the terminator [7] and sub-micrometer sized lunar dust particles are thought to travel as high as 100 kilometers from the lunar surface [8]. A similar (although opposite) behavior is believed to occur on the dark side of the Moon, where local electron fields cause the dust particles to become negatively charged. A dynamic fountain model has been developed to explain the movement of lunar dust particles as a result of environmental factors [8].

Additional regolith related environmental concerns include the size and morphology of lunar dust. Due to the absence of terrestrial erosion mechanisms (resulting in smoothing of particles found on Earth) in the lunar environment, the dust particles generally tend to have jagged edges and are generally highly abrasive and porous. Consequently, the dust poses significant problems to both manned and robotic missions. The ingress of jagged lunar dust particles into filter mechanisms and mechanical joints could compromise the efficiency and functionality of lunar outpost equipment. Apollo astronauts experienced great difficulty attempting to remove lunar dust that had contacted and adhered to their space suits and equipment [9]. Inhalation of lunar dust occurred during the Apollo 17 mission after the astronauts removed their space suits and resulted in respiratory distress [9]. To establish a long term presence on the Moon, it is clear that methods of avoiding dust contamination, and/or dust removal will be needed particularly in spacecraft and habitats.



*Figure 1.* Lunar missions requiring Extra-Vehicular Activity (EVA) during the Apollo missions were often complicated by the intrusion of lunar dust particles into the space suit material and equipment where its removal was hindered due to strong intermolecular forces. The above photo of astronaut Harrison Schmitt (Apollo 17) shows a layer of dust clinging to his space suit. NASA Photo: AS17-145-22157

Currently, several possible mitigation strategies are being considered that utilize the environmental properties of the Moon or regolith such as magnetism, electrostatic charges, etc. [5, 10] However, approaches that are scalable, practical, inexpensive, light weight and durable need to be identified and further developed.

One approach is to study how similar efforts have been effectively developed on Earth. Although researchers have demonstrated numerous dust resistant strategies using unique materials [11], electrostatic interactions [12], and specialized coatings [13]; nature has demonstrated a self-cleaning system that is not only remarkably efficient, but also has a physical basis that can be applied to other systems. This self-cleaning behavior is perhaps best demonstrated by the lotus plant, *Nelumbo Nucifera* [14].

Studies of lotus leaves and similar systems have determined that the lotus plant's self-cleaning ability (due to the observed superhydrophobicity of the leaves) is derived from two sources: surface chemical composition and surface topography [15]. The leaves of the lotus plant are able to remove adhered dust and debris due to the large contact-angle and small tilt angle of water incident on the leaves. A waxy material on the leaves is partially responsible for the observed low surface energy; however, the surface topography also contributes to this phenomenon. Topographical features on two different length scales--micrometer sized protuberances and nano-scaled surface textures--are what enable these natural materials to exhibit self-cleaning properties [16]. The micron sized features minimize the surface area of contact between the incident water droplet and the leaf, while the nanometer sized features either trap air pockets between the water and leaf surfaces (Cassie state) or amplify the hydrophobicity of the surface (Wenzel state) [17]. A number of researchers have demonstrated dual length-scale materials with high contact angles [18]. There is little to no water present in the lunar environment but reproduction of this surface topography on a space-durable material could result in a dramatic reduction of the surface contact area between regolith and surfaces of interest. Cohesion of lunar dust particles results predominantly from two intermolecular forces, van der Waals and Lewis acid-base interactions [3]. Reduction of the contact area would dramatically reduce the cohesive strength of the lunar regolith. The effects of surface roughness on mechanical interlocking are less intuitive. If the interacting particle possesses features much larger than those on the surface, mechanical interlocking would be minimized. If, instead, the particle was similarly sized to the larger topographical features of the surface, then the particle may interact very strongly with the surface. Clearly the mechanical interlocking of coarse particles on topographically-rich surfaces needs to be studied more extensively.

The work reported here used the polyhedral oligomeric silsesquioxane, octakis(dimethylsilyloxy)-silsesquioxane (POSS) to generate surface topography on polyimide films. This methodology demonstrates a facile way to generate and alter surface features (in an effort to reproduce lotus leaf topographical characteristics) for potential lunar dust resistance. The topography of these samples was modified by first "pretreating" the polyimide surface by exposure to oxygen plasma followed by spray-coating organic solution of POSS and additional oxygen plasma exposure. Surface characterization was conducted using optical microscopy and high-resolution scanning electron microscopy (HRSEM). Variation of the material's surface chemistry was monitored using infrared spectroscopy and energy dispersive spectroscopy (EDS).

Validation of this, and any, dust mitigation strategy requires several additional experimental procedures. For example, although there is no water vapor in the lunar atmosphere, contact angle measurements will be critical to evaluate the predominant surface interactions (i.e., dispersive, hydrogen bonding, acid-base, etc.) present. Likewise, actual dust interaction data

(e.g. abrasion resistance, cohesive interactions, electrostatic interactions) need to be determined and a dedicated vacuum chamber is being constructed at the NASA Glenn Research Center [19]. The degree of interaction of the exposed surfaces to lunar regolith will depend on the mobility of equipment and personnel at a lunar outpost and potentially on natural lunar regolith dynamics. With so many different types of potentially exposed surfaces and different mission requirements, it is unlikely that any single mitigation strategy will be applicable to every situation.

## 2. EXPERIMENTAL

**2.1 Materials** Kapton<sup>®</sup> HN (50.8 microns (2 mils), DuPont) was wiped with a dust-free cloth moistened with ethanol prior to surface treatments of any kind. Octakis(dimethylsilyloxy)silsesquioxane (POSS, Hybrid Plastics Inc.) was used as received. Oxygen plasma was created using a Plasma Prep<sup>™</sup> II Plasma Etcher (Structure Probes Inc.) at 100 W. Attenuated total reflection infrared (ATR-IR) spectra were recorded with a Thermo Nicolet IR300 spectrometer. Optical micrographs were collected using an Olympus BH-2 microscope equipped with a Hitachi KP-D50 digital color camera. HRSEM images were collected on a Hitachi S-5200 Field Emission High Resolution Scanning Electron Microscope equipped with a through the lens (TTL) detector and an EDS detector (EDAX, Mahwah, New Jersey). Due to poor conductivity and to enable EDS measurements (requiring > 10 kV), all SEM samples were sputter-coated with a ~10 nm thick gold/palladium film.

**2.2 POSS-coated Kapton<sup>®</sup> HN Sample Preparation** Kapton<sup>®</sup> HN samples were exposed to oxygen plasma to “activate” the Kapton<sup>®</sup> HN surface prior to POSS deposition. Initial experiments were conducted without this pretreatment activation step and resulted in highly heterogeneous POSS surface coverage (likely due to the low surface free energy of Kapton<sup>®</sup> HN). Therefore, all samples were exposed to oxygen plasma prior to POSS deposition. Exposure times were varied between 30 min and 2 h with 1 h determined to provide the best results (i.e. leading to more uniform wetting). POSS was deposited on Kapton<sup>®</sup> HN surfaces from a 1 wt % THF solution using a Badger Model 250 mini spray gun in consecutive treatments, allowing the THF to evaporate between passes. The typical Kapton<sup>®</sup> HN sample size was a 5 cm × 5 cm square. For oxygen plasma exposure, specimens were placed in the middle of the plasma exposure area to achieve a more uniform exposure to molecular oxygen. Once pretreated samples were removed from the plasma chamber, POSS deposition was performed within 30 sec to prevent deactivation of the Kapton<sup>®</sup> HN surface from ambient moisture. Samples were then exposed to oxygen plasma in 30 min increments up to the specified cumulative time. Kapton<sup>®</sup> HN samples were exposed to oxygen plasma for the same duration as POSS-coated Kapton<sup>®</sup> HN samples to compare and characterize the exposure effects on the topography of the two surfaces.

## 3. RESULTS AND DISCUSSION

**3.1 Material Surface Modification** This approach towards the development of a space-durable material with dual length-scale surface topographical features requires the use of a combination of highly aromatic organic materials and relatively inert inorganic compounds. To this end, Kapton<sup>®</sup> HN [a polyimide generated from the condensation of pyromellitic dianhydride and bis(4-aminophenyl)ether] was selected because of its widespread use in a variety of space

missions. Polyimides in general, possess low moisture uptake, good insulating properties, excellent thermal stability, and good mechanical properties [20].

Although there are several inert inorganic materials that could generate tailorable dual length scale surface topographies for lunar dust mitigation (silica microparticles [21], nanotubes of several compositions [22]) only POSS will be discussed here. POSS has been effectively added to polymeric systems for various purposes [23]. When POSS is used as a filler in nanocomposite systems or in the backbone of polymerization reactions the resultant materials often demonstrate enhanced physical and mechanical properties [24].

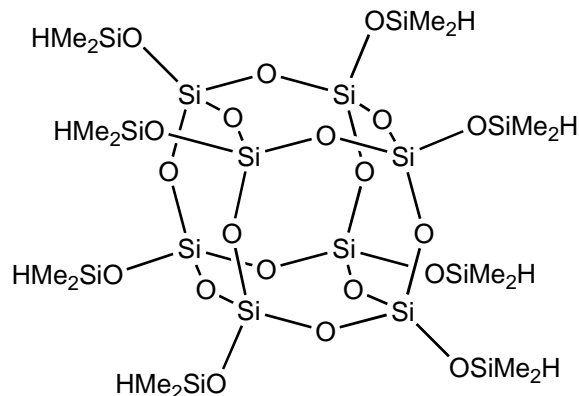
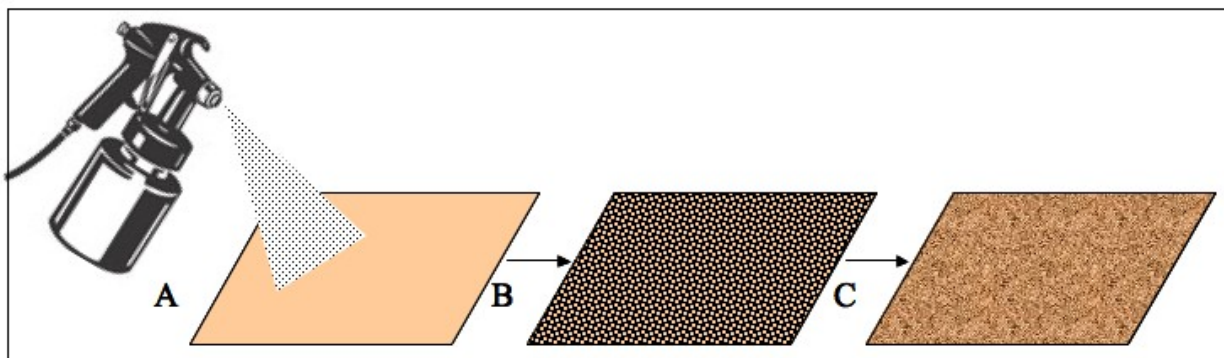


*Figure 2.* Structure of octakis(dimethylsilyloxy)silsesquioxane.

POSS molecules are cube-like structures with silicon atoms at the corners connected by oxygen atoms. The resultant POSS structure can be empirically written as  $\text{SiO}_x$ , where  $x = 1.5$  (for silicones and silica  $x = 1$  and  $2$  respectively). This intermediacy imbues POSS with unique properties, such as atomic oxygen resistance [25]. The architecture of POSS molecules allows for the incorporation of an array of functionalities. Aside from using incomplete POSS cages for reactions, each corner Si atom has an additional bonding site that can be chemically modified. For this work, the reactive site was occupied by a dimethylsilyloxy  $[-\text{OSi}(\text{Me})_2\text{H}]$  group (Figure 2). It was anticipated that the highly reactive silane bond (Si-H) would react with chemical functionalities generated on the polyimide film surface by oxygen plasma activation.

**3.2 Sample Preparation** Different treatment protocols used in this study resulted in dramatically different surface topographies. Pretreatment of the Kapton<sup>®</sup> HN surface with oxygen plasma for 1 h dramatically reduced the pooling of sprayed THF droplets, compared to non-pretreated surfaces. When relatively large amounts of solution were deposited in a single treatment, solvent droplets would coalesce resulting in large pools, subsequently yielding less uniform POSS deposition. Several small volume deposition cycles enabled relatively homogeneous POSS deposition. Exposure of Kapton<sup>®</sup> HN to oxygen plasma results in reactive surface group formation (ketone, aldehyde, ester, and carboxylic acid functionalities arise from bond scission and insertion processes) [26] which have the potential to react with the POSS silane bonds present on the POSS molecule.

Scheme 1. POSS-coated Kapton<sup>®</sup> HN sample preparation methodology. Kapton<sup>®</sup> HN surfaces are pretreated by exposure to oxygen plasma (A). Organic solutions of POSS are sprayed on the surfaces generating surface topographies (B). This surface is altered by additional oxygen plasma exposure (C).



Regardless of oxygen plasma pretreatment time, the surface is most likely covered with chemically bound and physi-sorbed POSS molecules. To study the feasibility of altering the surface topography of POSS-coated Kapton<sup>®</sup> HN, samples were subjected to additional oxygen plasma exposure after POSS deposition. Visually the samples appeared hazy (diffuse) around POSS deposits after as little as 30 min of additional oxygen plasma exposure. After long exposure times (5 h), the samples showed signs of loss of material (thinning of the film near the sample edges or disappearance of film sections altogether).

**Table 1.** POSS coated Kapton<sup>®</sup> HN Oxygen Plasma Exposure Times.

Sample	Oxygen Plasma Exposure Time (min)	
	Prior to POSS deposition	After POSS deposition
I	60	--
II	30	30
III	60	30
IV	60	60
V	60	120
VI	60	240
VII	60	300

**3.3 ATR-IR Characterization** Each POSS molecule possesses eight reactive silane (Si-H) bonds. Exposure to oxygen plasma can initiate two different chemical reaction pathways. First, the Kapton<sup>®</sup> HN surface could undergo further oxidation or react with the Si-H bonds of the POSS molecules. Secondly, exposure to oxygen plasma could result in direct oxidation of either

the Si-H bonds or POSS cages themselves resulting in surface materials with chemical formulas approaching silica (e.g. passivation).

The disappearance of Si-H stretching vibrations can be monitored as a function of oxygen plasma exposure via ATR-IR. In an effort to assess the degree of Si-H bond reaction, ratios were calculated from two characteristic octakis(dimethylsilyloxy)silsesquioxane vibrations, the Si-H stretch ( $\nu = 2140 \text{ cm}^{-1}$ ) and the Si-O-Si stretch ( $\nu = 1068 \text{ cm}^{-1}$ ), as a function of oxygen plasma exposure time. These IR-active modes were chosen because they involve the functional group of interest, the Si-H bond, and are resolved from the spectral features of Kapton<sup>®</sup> HN. There is a dramatic reduction in the Si-H stretch intensity upon extended oxygen plasma exposure of POSS-coated Kapton<sup>®</sup> HN samples (Figure 3). After 1 h, there appears to be a negligible amount of Si-H bonds remaining (possibly indicating a maximal time of non-destructive oxygen plasma induced topographical modification for the loading levels used here). One possible complication with this analysis is that the number of Si-O-Si bonds could increase as a result of oxygen plasma exposure and resultant POSS decomposition. It is not possible to differentiate between the disappearance of Si-H bonds and generation of Si-O-Si bonds in these spectra due to overlap of other diagnostic POSS vibrational features and Kapton<sup>®</sup> HN contributions. However, it is probable that the formation of Si-O-Si features could arise partly from the reaction of Si-H functionalities.

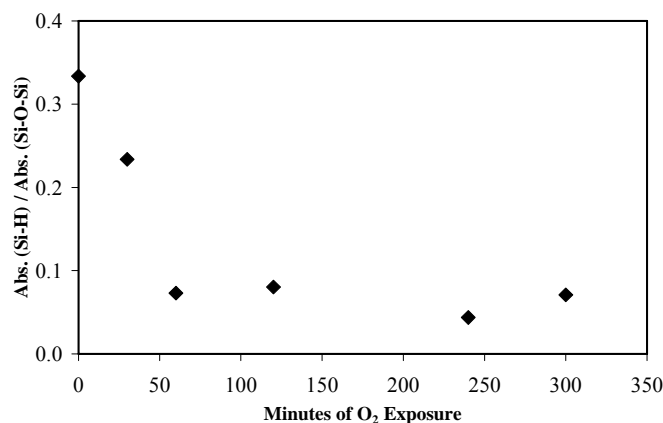


*Figure 3.* Ratios of the absorbance determined for Si-H and Si-O-Si bands using ATR-IR spectroscopy indicate a rapid disappearance of Si-H bands as a result of exposure to oxygen plasma. After 1 h, additional oxygen plasma exposure does not dramatically reduce this ratio suggesting that a majority of the POSS molecules have reacted in the oxygen plasma.

**3.4 Microscopic Characterization** Both optical microscopy and HRSEM were used to observe the effects of oxygen plasma exposure on the surface topography of POSS-coated Kapton<sup>®</sup> HN samples. Poor electrical conductivity of both POSS and Kapton<sup>®</sup> HN required sputter-coating of the samples with Au/Pd (~ 10 nm thick) for HRSEM imaging. One unfortunate consequence of this treatment is that surface features  $\leq 10 \text{ nm}$  can be affected by the sputter coating process making it impossible to determine the source of these features.

**3.4.1 Oxygen Plasma Exposure Effects on Kapton<sup>®</sup> HN** The damaging effects of long-term oxygen plasma exposure on Kapton<sup>®</sup> HN are well documented [27]. To delineate the effects of

oxygen plasma exposure on Kapton<sup>®</sup> HN and POSS architectures, images were collected of Kapton<sup>®</sup> HN exposed to oxygen plasma without POSS deposits. Oxygen plasma exposure enhances the surface roughness of Kapton<sup>®</sup> HN, with roughness increasing with exposure time. Kapton<sup>®</sup> HN exposed to oxygen plasma for 60 minutes (Figure 4B) results in the formation of small spherical structures (5 – 15 nm) and aggregate structures (35 – 60 nm). Extended exposure (90 minutes, Figure 4C) predominantly reveals single particulates on the surface with populations in two different size regimes, 15 – 30 nm and 50 – 70 nm.

At long exposure times (5 h), complete degradation of the sample is observed near the sample edges and small holes were observed throughout the sample. Introduction of these holes may be due to local surface defects increasing surface free energy enhancing surface reactivity. Similarly, residual organic debris from reaction with the oxygen plasma, covers large portions of the surface (Figure 4D). The presence of this organic residue provides some protection for the underlying Kapton<sup>®</sup> HN, while the surrounding polymeric material continues to etch away due to differences in erosion rates. The size of these pockets varies greatly (100 nm – 3  $\mu$ m) with smaller sized pockets more heavily populating the surface.

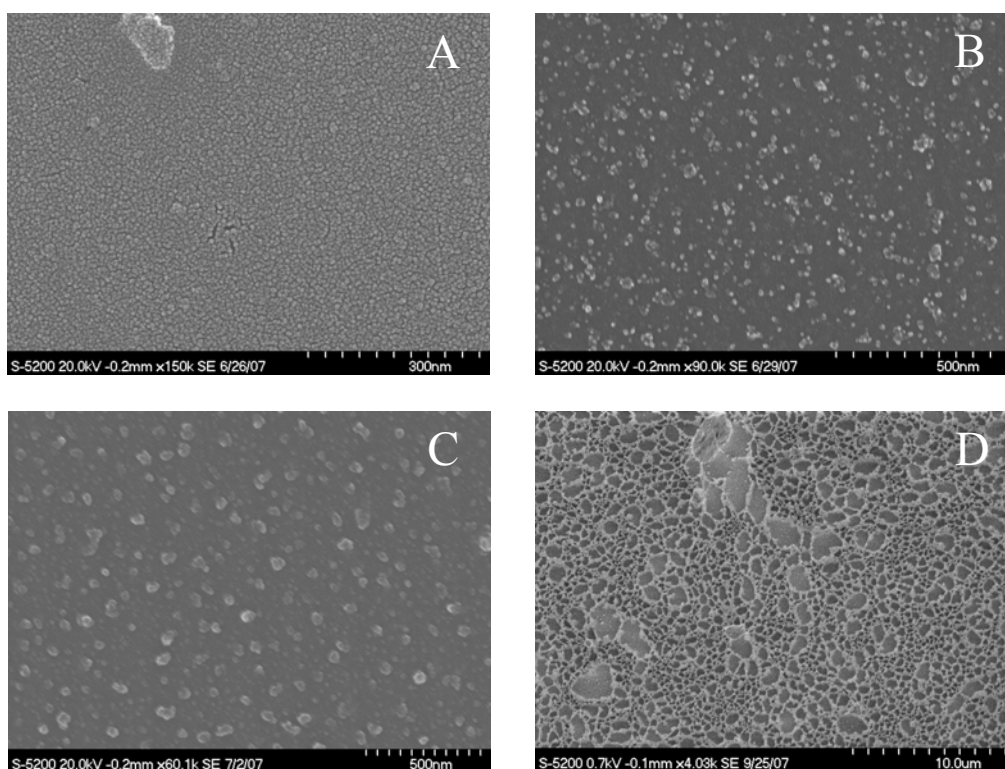


*Figure 4.* HR-SEM images of “neat” Kapton<sup>®</sup> HN with exposure to oxygen plasma for 0 min (A), 60 min (B), 90 min (C), and 5 h (D). The introduction of surface topography due to Au/Pd sputtering can be seen in A. Exposure to oxygen plasma results in the appearance of surface features larger than the sputter material (B and C). The size of these features increases with exposure time. Continued exposure to oxygen plasma resulted in the formation of a network of organic debris that appears to be atomic oxygen resistant (D). Regions not covered by this surreptitiously created protective layer continued to be etched away and shared a topography similar to C.

**3.4.2 Resultant Topography of POSS Deposition** When POSS is deposited on pretreated Kapton<sup>®</sup> HN, “fern-like” structures (10 – 100  $\mu\text{m}$ ) are observed to be the dominant surface feature with “arms” extending from “fern” stems (Figures 5 – 7). Areas with high concentrations of POSS appear as stacked ferns. Large circular POSS deposits, both irregular and uniform in appearance, are also observed with diameters of 10 – 50  $\mu\text{m}$  typically (although circular topographies as large as 100  $\mu\text{m}$  were observed). Although the currently investigated POSS deposition amounts do not result in uniform surface coverage, the resultant topography is increased in homogeneity compared to non-pretreated Kapton<sup>®</sup> HN surfaces (data not shown). EDS analysis confirmed the composition of the introduced topographical features to be POSS as indicated by enriched silicon and oxygen and diminished carbon mapping (Figure 7).

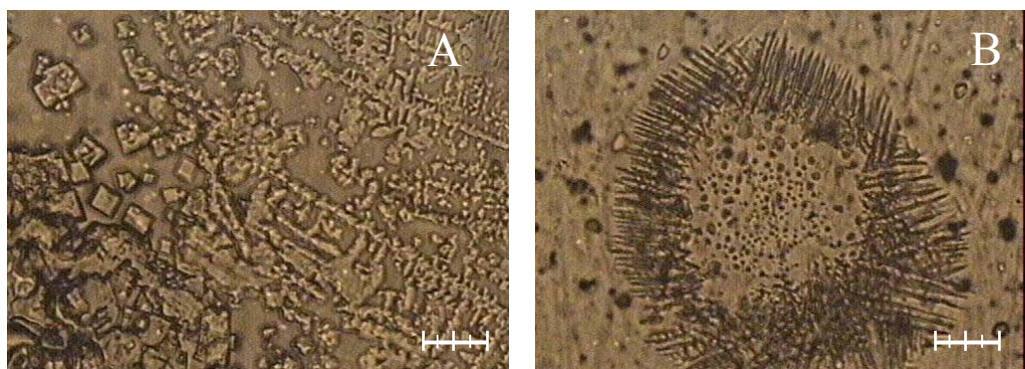


*Figure 5.* Optical photomicrographs of sample I. Long, slender “fern-like” features are predominantly observed on the surface. Areas of high POSS concentration also exhibit small cubes or large platelets. Occasional circular deposits are observed as well. The scale bar in both images is 20  $\mu\text{m}$ .

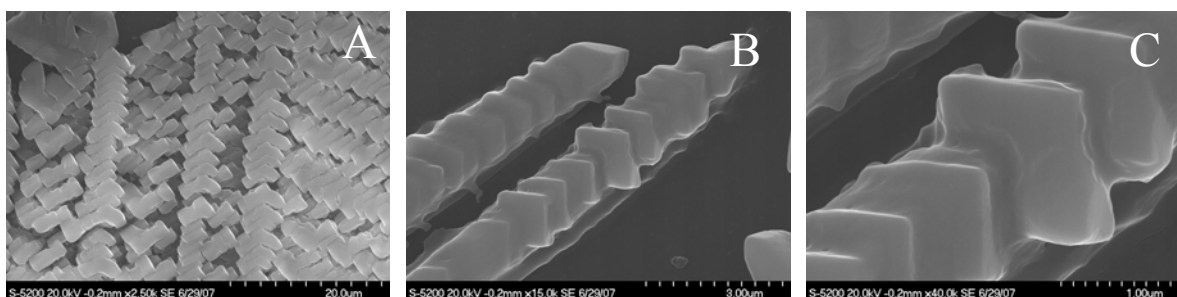


*Figure 6.* Fern-like structures are observed in areas of high POSS concentration and form large POSS aggregates which appear to consist of a collection of “brick” and “boomerang” type structures (A). The discrete bricks are dimensionally consistent (4  $\mu\text{m}$  by 2  $\mu\text{m}$ ). Bricks are frequently fused together forming the “arms” of the fern-like structures (B). The fused rectangular structures (C) are quite uniform, 1.0 – 1.5  $\mu\text{m}$  long with approximately 750 nm of separation between rectangles. The thickness of the arms is generally 1.5  $\mu\text{m}$ . All images are of sample I.

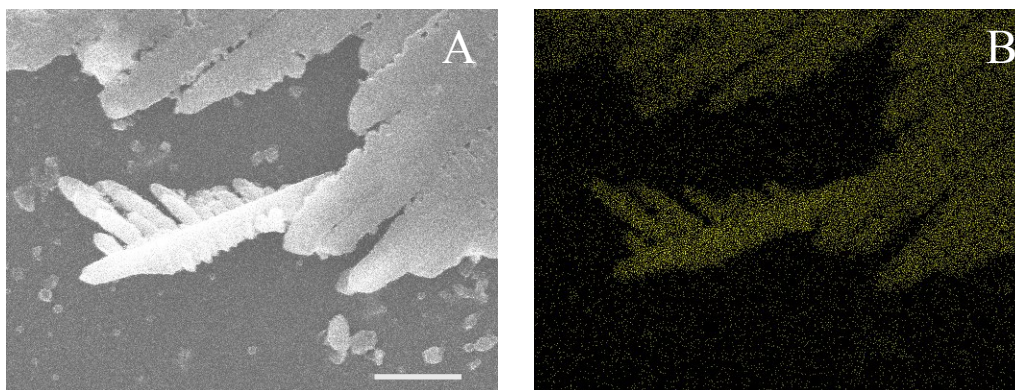


*Figure 7.* The “fern” structures observed on sample I (A) are clearly traced out in the silicon EDS map (B). The oxygen map was similarly enriched while the carbon map was depleted in the areas exhibiting POSS deposit features (data not shown). The small spherical particles in A do not appear on the Si map and are likely to arise from the Kapton<sup>®</sup> HN itself as seen in Figure 4C. The scale bar in A is 5  $\mu\text{m}$ .

**3.4.3 Surface Modification of POSS-coated Kapton<sup>®</sup> HN** Oxygen plasma exposure of POSS-coated Kapton<sup>®</sup> HN samples results in growth of tendrill-like topographical features (Figure 8). The presence and length of these observed topographies appears to increase with oxygen plasma exposure time. The appearance of these features radiating from POSS deposits suggest that the silicate surface coverage is expanding due to oxygen plasma exposure. This may result in uniform surface coverage of Kapton<sup>®</sup> HN if the initial POSS deposition amount is sufficient. It is unclear what mechanism would cause POSS to migrate from regions of high POSS concentrations to regions of low POSS concentrations and conditions for homogeneous POSS surface coverage are currently being evaluated.

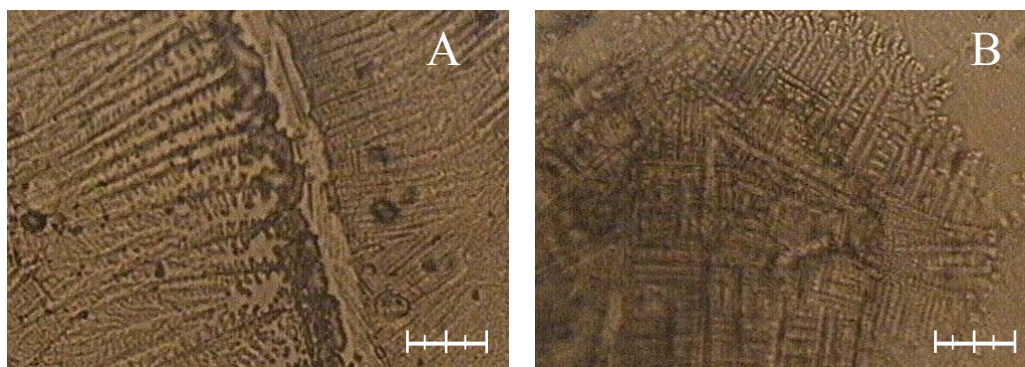


*Figure 8.* Sample II demonstrates tendrill growth from existing POSS deposits of both fern (A) and circular (B) architectures due to oxygen plasma exposure. The scale bar in both images is 20  $\mu\text{m}$ .

A broad expanse of fern-like POSS deposits is seen in the HRSEM image of sample III in Figure 9A. Closer inspection reveals a surface with three distinct regions (Figure 9B). The brightest region clearly corresponds to POSS deposits. These features are 200 – 400 nm thick

and exhibit peak-like structures in the middle or at intersections possibly due to restructuring caused by exposure to oxygen plasma. The space surrounding these POSS deposits appears to be Kapton<sup>®</sup> HN that has eroded due to oxygen plasma exposure. This region generally follows the contour of the POSS deposits and is similar in dimension (250 – 450 nm). Undercutting of the POSS deposits is also observed; similar to what has been observed previously [28]. The POSS/Kapton<sup>®</sup> HN interface is likely an area with enhanced oxygen plasma erosion rates due to increased surface free energy. Finally, there is a region between the areas of enhanced Kapton<sup>®</sup> HN erosion that appears to be covered with a thin layer of silicate.

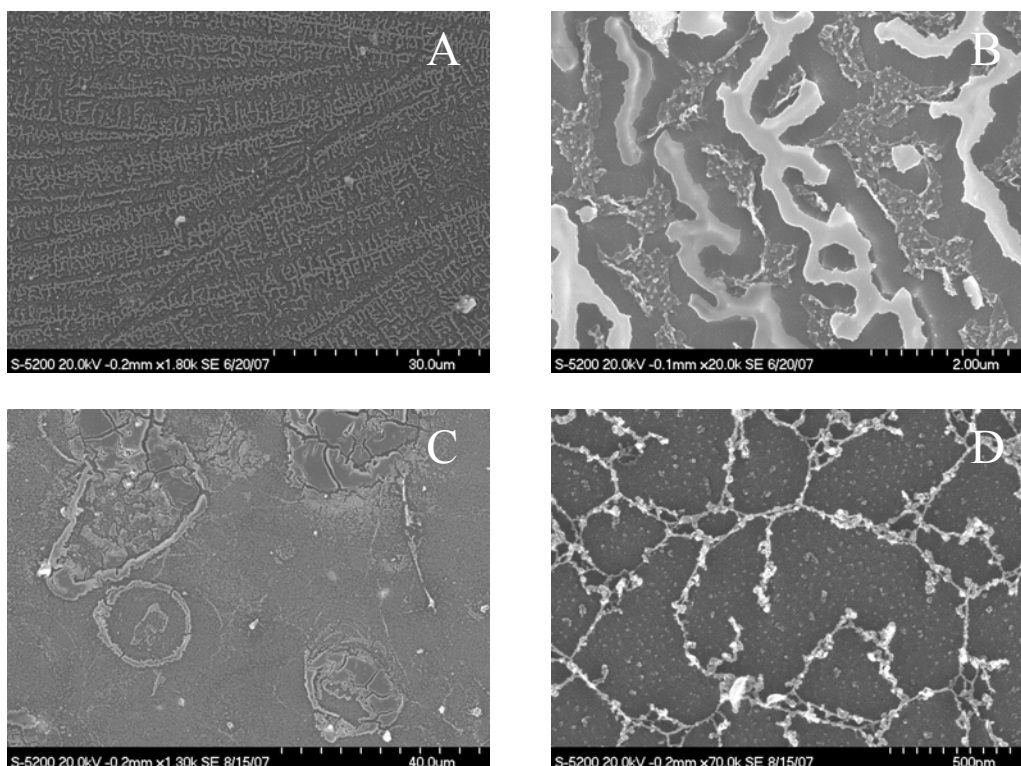


*Figure 9.* HRSEM images of samples III (A and B, where B is a magnified view of the structures seen in A) and IV (C and D). Initial stages of tendrill growth can be seen after only 30 min of oxygen plasma exposure with 1 h resulting in dramatic surface coverage and introduction of new topographical features.

Further exposure to oxygen plasma results in continued spreading of this triphasic surface (Figure 9C taken of sample IV). This expansion could be due to evaporation/condensation processes initiated by oxygen plasma exposure. Tendril structures (Figure 9D,  $8 \pm 2$  nm thick with intersection of features resulting in increased thickness) appear after much shorter oxygen plasma exposure times compared to the similar surface topographies observed for neat Kapton<sup>®</sup> HN (see Figure 4D). However, they seem to provide the same form of limited protection. In the upper right corner of Figure 9C, a circular POSS deposit appears to have formed cracked platelets covering the Kapton<sup>®</sup> HN surface generating a more uniform surface coverage.

Additional exposure to oxygen plasma results in apparent smoothing of the surface topography of POSS deposits: the upper region of both the large circular deposits and fern-like deposits appears to become smoother (Figure 10). The arms comprised of fused rectangular

features (as shown in Figure 6) have been reduced to nearly featureless arms (2 – 4  $\mu\text{m}$ ) protruding from central fern stems (6 – 8  $\mu\text{m}$ ). Rough surface structures should be the most reactive due to enhanced surface free energy associated with surface defects. Exposure to oxygen plasma also appears to meld adjacent arms.

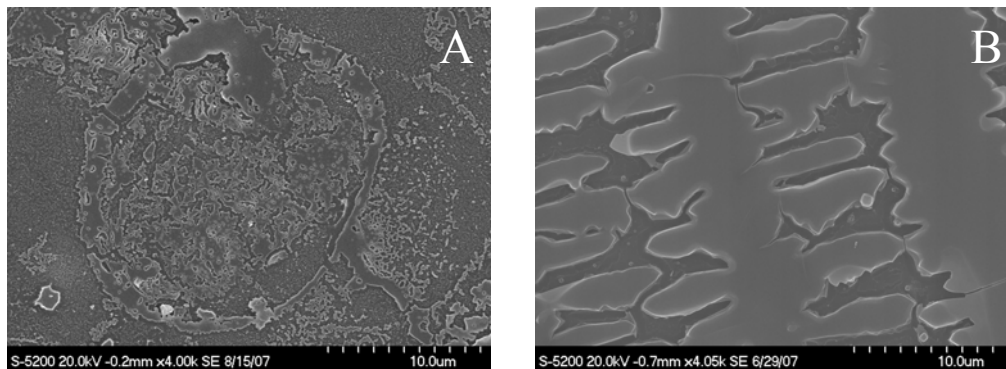


*Figure 10.* Exposure to oxygen plasma results in smoothing of both the exterior and interior features of the large circular deposits (sample V, A) and the fern structures (sample II, B).

Alteration of the POSS deposit topography due to oxygen plasma exposure results in modification of the POSS features and expansion of the POSS-coated regions. These changes have two effects. First, oxygen plasma exposure appears to advance these surfaces towards more uniform POSS surface coverage (i.e. uniform as in consistent POSS surface concentration and not in terms of topographical architecture.) Second, topographical features that were modified or generated as a result of oxygen plasma exposure resemble dual length scale properties where large POSS deposits (micrometers to hundreds of nanometers) are surrounded and possibly covered with smaller, nanometer sized, features. In some cases, nanometer sized features seem to be removed by oxygen plasma exposure (Figure 10B). The potential influence of the sputter-coating process prevents discussion of topographies on a smaller length scale.

**3.4.4 Detrimental Effects of Oxygen Plasma Exposure on POSS-Coated Kapton<sup>®</sup> HN** Long-term ( $\geq 2$  h) oxygen plasma exposure on POSS-decorated Kapton<sup>®</sup> HN surfaces results in additional topographical modifications. Holes are developed in POSS deposits ( $< 400$  nm) and large sections of the deposits (up to 1  $\mu\text{m}$ ) appear removed as oxygen plasma exposure times increased (Figure 11A and B). It is highly likely that holes in the POSS deposits allow degradation of the underlying Kapton<sup>®</sup> HN substrate. “Fern” stems and “arms” are reduced in size ( $800 \pm 50$  nm and  $500 \pm$  nm, respectively) compared to deposits without oxygen plasma exposure ( $1500 \pm 150$  nm and  $1000 \pm 250$  nm, respectively). Fusion of adjacent platelets also results in formation of relatively uniform circular POSS deposits (Figure 11 C), compared with the cracked platelets observed in Figure 9C. Collectively, all of the discussed topographical features suggest that, at appropriate surface concentrations, spray-deposition of POSS can effectively produce a tailorable, topographically rich surface.

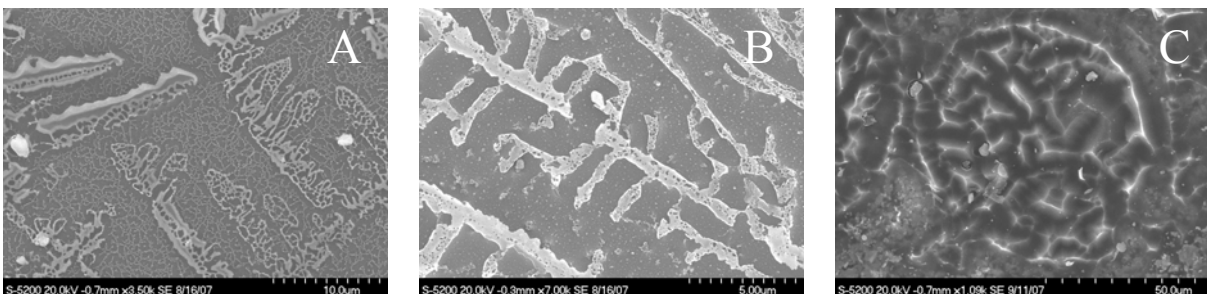


*Figure 11.* HRSEM images of samples VI (A), VII (B), and VIII (C). The tendril network appears to cover a majority of the surface after only 2 h of oxygen plasma exposure. After 4 h, the fern-like POSS structures display holes and structural degradation. Fusion of the platelets covering circular deposits observed on the surface of sample IV is observed after 5 h generating structures that cover large areas of the substrate.

## 4. CONCLUSION

Kapton<sup>®</sup> HN substrates were coated with POSS molecules to develop materials capable of topographical modification via oxygen plasma exposure. Analytical techniques enabled the determination of not only the behavior of POSS molecules diffusing from THF solution to the Kapton<sup>®</sup> HN surface, but also changes in topography and chemistry as a result of oxygen plasma exposure. The methodology described here successfully produced materials with both micro- and nano-scaled topographical features. This approach is applicable to a variety of polymeric materials.

## 5. ACKNOWLEDGEMENTS

The authors would like to thank Dr. Peter Lillehei for scientific and technical support and the NASA post-doctoral program by Oak Ridge Associated Universities.

## 6. REFERENCES

1. *NASA's exploration systems architecture study*, NASA/TM--214062,
2. Gaier, J., *The effects of lunar dust on EVA systems during the apollo missions*, NASA/TM--213610, 2005.
3. Lee, Lieng-Huang, *J. Adhes. Sci. Technol.*, **9**, 1103 (1995).
4. Carrier, W. David, Olhoeft, Gary R., et al., *Lunar sourcebook: A users guide to the Moon*, Cambridge University Press, 1991.
5. Taylor, Lawrence and Meek, Thomas, *J. Aerospace Eng.*, **18**, 188 (2005).
6. Borisov, N. and Mall, U., *Planetary Space Sci.*, **54**, 572 (2006); Kolesnikov, E. and Yakovlev, A., *Planetary Space Sci.*, **51**, 879 (2003).
7. Rennilson, J. and Criswell, D, *The Moon*, **10**, 121 (1974).
8. Stubbs, Timothy;, Vondrak, Richard;, et al., *Adv. Space Res.*, **37**, 59 (2006).
9. Goodwin, R., *Apollo 17: The NASA mission reports*, Apogee Books, Ontario, Canada, 2002.

10. Immer, C., Starnes, J., et al., Lunar and Planetary Science XXXVII, (2006); Proctor, Margaret P. and Dempsey, Paula Survey of dust issues for lunar seals and the resolve project NASA/TM--0010457 2006.
11. J.P. Pat. 2006020552 Fujiwara, Katsuhiko, Takasawa, Takashi, et al. (to the (MKV Platech Co., Ltd., Japan).); U. S. Pat. 4395443 (Jul. 26, 1983) Shimizu, C. and Hosokowa, K. (to the Toshiba Silicones Ltd., Japan)
12. U.S. Pat. 2004055632 (Mar. 25, 2004) Mazumder, Malay K., Sims, Robert A., et al. (to the (Board of Trustees of the University of Arkansas, USA).); U.S. Pat. (May 2, 2000) Venzant, K. (to the BRK Brands, Inc., Aurora, Ill.)
13. United States 4208496 (Jun. 17, 1980) Bergfeld, R., Patel, S., et al. (to the N. L. Industries Inc., New York); U.S. Pat. 5846646 (Dec. 8, 1998) Meppelink, R., Renault, P., et al. (to the Levolor Corporation, Sunnyvale, CA); U.S. Pat. 6299721 (Oct. 9, 2001) Poutasse, C. and Centanni, M. (to the Gould Electronics Incl., Eastlake, OH); U.S. Pat. 4511489 (Apr. 16, 1985) Requejo, L. and Butke, C. (to the The Drackett Company, Cincinnati, OH)
14. Barthlott, W. and Neinhuis, C., Planta, 202, 1 (1997).
15. Neinhuis, C. and Barthlott, W., Ann. Botany, 79, 667 (1997).
16. Patankar, Neelesh A., Langmuir, 20, 8209, (2004).
17. Callies, M. and Quere, D., Soft Matter, 1, 55 (2005).
18. Chen, S., Hu, C., et al., Chem. Commun., 1919 (2007); Furstner, Reiner, Barthlott, Wilhelm, et al., Langmuir, 21, 956, (2005); Zhang, L., Zhou, Z., et al., Langmuir, 22, 8576 (2006).
19. Gaier, James and Sechkar, Edward, Lunar simulation in the lunar dust adhesion bell jar, NASA/TM--214704, 2007.
20. Polyimides, Chapman and Hall, New York, 1990.
21. Zhang, Yilei and Sundararajan, Sriram, Langmuir, 23, 8347 (2007).
22. Li, Y., Huang, X. J. , et al., Langmuir, 23, 2169 (2007).
23. Tegou, Evangelia, Bellas, Vassilios, et al., Chem. Mater., 16, 2567 (2004); Wright, Michael, Schorzman, Derek, et al., Chem. Mater., 15, 264 (2003); Wu, Shouming, Hayakawa, Teruaki, et al., Macromolecules, 40, 5698 (2007).
24. Bian, Yu, Pejanovic, Srdjan, et al., Macromolecules, 40, 6239 (2007); Pan, Guirong, Mark, James, et al., J. Polym. Sci., Part B: Polym. Phys., 41, 3314 (2003); Phillips, Shawn, Haddad, Timothy, et al., Curr. Opin. Solid State Mater. Sci., 8, 21 (2004).
25. Augustine, Brian, Hughes, Wm. Christopher, et al., Langmuir, 23, 4346 (2007); Brunsvold, A. L., Minton, T., et al., High Perform. Polym., 16, 303 (2004); Gilman, Jeffrey, Schlitzer, David, et al., J. Appl. Polym. Sci., 60, 591 (1996); 26. Chan, C. M., Polymer surface modification and characterization., Carl Hanser Verlag, Munich, 1994.
27. A. Levine LDEF--69 Months in Space: First Post Retrieval Symposium, NASA -CP, 3134 (2) (1992); A. Levine LDEF Second Post Retrieval Symposium, San Diego CA, NASA-CP 10097 (1992); Gerlach, L., Ecol. Soc. Amer., 14, 149, (1990); Hansen, R., Pascale, J., et al., J. Polym. Sci., Part A: Polym. Chem., 3, 2205 (1965); Leger, J., NASA/TM--58246, 1982; Leger, L., Visentine, J., et al., SAMPE Quarterly, 18, 48 (1987); Stein, B., LDEF Materials Workshop-91, NASA-CP 3162 (1) (1991); Visentine, J., NASA/TM--100459 (1-2), 1988; Zimcik, D. and Maag, C., Journal of Spacecraft, 25, 162 (1988); Snyder, A., Investigation of atomic oxygen erosion of polyimide kapton h exposed to a plasma asher environment, NASA/TM--209178, 1999.
28. de Groh, K. and Banks, B., Journal of Spacecraft and Rockets, 31, 656 (1994); Rutledge, S. and Mihelcic, J., Surf. Coat. Technol., 39/40, 607 (1989).